Quantitative microcomputed tomography analysis of mineralization within three-dimensional scaffolds *in vitro*

Sarah Cartmell, Kimberly Huynh, Angela Lin, Srinidhi Nagaraja, Robert Guldberg
School of Mechanical Engineering, IBB Building, 315 Ferst Drive, Georgia Institute of Technology, Atlanta, Georgia 30332

Received 4 April 2003; revised 23 October 2003; accepted 6 November 2003

Abstract: Synthetic and naturally derived scaffold biomaterials in combination with osteogenic cells or bioactive factors have the potential to serve as bone graft substitutes. Porous poly(l-lactide-*co*-dl-lactide) (PLDL) scaffolds with mechanical properties comparable to trabecular bone and an oriented, interconnected porosity designed to enhance internal mass transport were recently developed. In this study, PLDL scaffolds were seeded with rat calvarial or rat stromal cells and cultured up to 8 weeks in media containing osteogenic supplements. Cell-seeded human demineralized trabecular bone matrix (DTBM) scaffolds were included for comparison. All constructs were imaged weekly from 4 to 8 weeks using microcomputed tomography (micro-CT) to nondestructively quantify the amount and distribution of mineralized matrix formation. The total mineralized matrix volume increased with time in culture for all construct groups. DTBM constructs contained significantly more mineralized matrix than PLDL constructs. However, an analysis of the acellular DTBM scaffolds exposed to osteogenic media revealed partial remineralization of the demineralized matrix whereas no mineralization was detected in acellular PLDL scaffolds. Differences in mineral distribution were also evident with cell-mediated mineralization found throughout the PLDL constructs but localized to the periphery of the DTBM constructs for both cell types. Expression of bone marker genes indicating osteoblast differentiation was demonstrated in all groups at 8 weeks using a quantitative reverse transcription polymerase chain reaction. Osteocalcin expression was significantly higher for calvarial cell constructs compared to stromal cell constructs, regardless of the type of scaffold. This study demonstrated that micro-CT imaging may be used to nondestructively and quantitatively monitor mineralization within three-dimensional scaffolds *in vitro*. PLDL scaffolds with an oriented microarchitecture were shown to support cell attachment, differentiation, and cell-mediated mineralization comparable to natural DTBM scaffolds. © 2004 Wiley Periodicals, Inc. J Biomed Mater Res 69A: 97–104, 2004

Key words: computed tomography; bone tissue engineering; mineralization; polylactides

INTRODUCTION

The clinical need for bone graft substitutes is well established.[1,2] Autogenous bone grafting is currently the clinical standard for osseous reconstruction. However, the use of autograft bone has several disadvantages including limited available tissue for transplantation, lack of structural integrity to withstand functional loads, and increased patient morbidity. Structural bone allografts are available, but they are associated with an increased risk of disease transmission and a decreased ability to stimulate repair. Demineralized bone matrix was first used as a bone graft substitute in 1889,[3] and it has since been shown to be osteoinductive *in vivo*[4–6] and is now widely used clinically to augment bone repair.[7–9]

In addition to demineralized bone matrix, numerous other synthetic and naturally derived porous scaffolds are being developed as bone graft substitutes and delivery vehicles for osteogenic cells and bioactive factors.[10–18] However, bone repair scaffolds are typically limited by inadequate mechanical properties to withstand functional loading *in vivo*. We have recently developed porous poly(l-lactide-*co*-dl-lactide) (PLDL, 70:30 l-lactide/dl-lactide) scaffolds with mechanical properties comparable to trabecular bone using a solution coating and porogen decomposition technique.[19] The polymer scaffolds also possess a unique microarchitecture characterized by axially oriented macroporosity coupled with randomly interconnected microporosity.

In vitro three-dimensional (3D) culture has previ-

Correspondence to: R. E. Guldberg; e-mail: robert.guldberg@me.gatech.edu

Contract grant sponsor: National Science Foundation; contract grant number: EEC-9731643
Contract grant sponsor: Wellcome Trust

ously been used to evaluate the potential for various scaffold materials and microarchitectures to support cell attachment and mineralized matrix formation. For example, Ishaug-Riley et al. described the production of bonelike tissue *in vitro* by rat calvarial cells cultured for 56 days on a 90% porous polymeric scaffold.[15] The presence and distribution of mineralized matrix has typically been assessed qualitatively using Von Kossa fast green (VK) staining for phosphate deposits on 2D histological sections.[15,20] However, this approach is destructive and does not necessarily provide an accurate representation of mineralization throughout the 3D construct.

Microcomputed tomography (micro-CT) imaging and analysis has been used extensively to characterize the 3D trabecular bone microarchitecture and quantify bone repair responses *in vivo*.[21–23] For tissue engineering applications, micro-CT imaging may provide an efficient, nondestructive tool to quantitatively measure the amount and distribution of mineralized matrix formation throughout 3D constructs *in vitro* and *in vivo*. The first objective of this study was to monitor matrix mineralization within 3D scaffolds over time and determine the effect of repeated micro-CT imaging on cellular function. The second objective was to compare the amount and distribution of *in vitro* mineralized matrix production within oriented PLDL scaffolds and demineralized trabecular bone scaffolds with similar porosity.

MATERIALS AND METHODS

Scaffold preparation

PLDL scaffolds were prepared as described previously.[19] Briefly, a solid mixture of 80% PLDL (70% l-lactide, 30% dl-lactide, inherent viscosity = 4.86 dL/g; Purac America, Lincolnshire, IL) and 20% azodicarbonamide (pore-forming substance; Aldrich, Milwaukee, WI) was dissolved in acetone. Then, 316 stainless steel wires (100-μm diameter; California Fine Wire, Grover Beach, CA) were coated with this solution. The coated wires were cut, bundled, and heated in a 120°C oven until the wires bonded. To create the porous structure, the bundle was then heated in 260°C peanut oil, decomposing the porogen agent and producing randomly oriented microporosity. After rinsing in hexane, the wires were removed, revealing axially oriented macropores. Finally, the scaffolds were cut into disks (ϕ = 6 mm, height = 3 mm) and sterilized using γ radiation (2.5×10^6 rad). The average porosity of the PLDL scaffolds was 71.5 ± 1.6% and the average pore size was 318.0 ± 12.1 μm, as measured by micro-CT analysis (Micro-CT 40, ScanCo Medical). An evaluation of the PLDL scaffold degradation kinetics indicated a less than 10% mass loss and no significant change in the mechanical properties over the 8-week course of *in vitro* experiments.

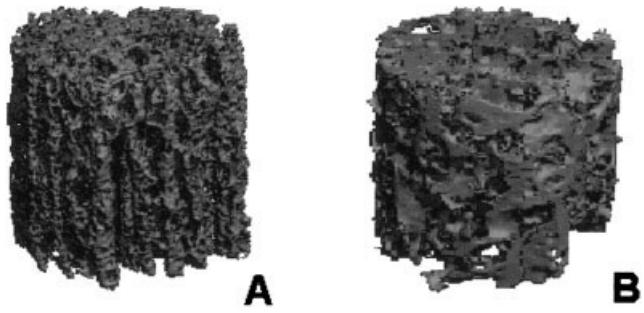

Figure 1. Representative micro-CT images of (A) PLDL and (B) undemineralized trabecular bone scaffolds prior to seeding.

Sterile freeze-dried human trabecular bone samples (Georgia Tissue Bank) were hydrated for 1 h in sterile phosphate buffered saline (PBS) and cut into cylinders (ϕ = 6 mm, height = 3 mm). Prior to decalcification, all bone scaffolds were imaged at a voxel resolution of 16 μm to record the initial scaffold morphology (Fig. 1). The average porosity of the bone scaffolds was 79.9 ± 5.1% and the average pore size was 598.5 ± 74.5 μm. The bone samples were then decalcified with a 20% sodium citrate and 44% formic acid solution, which was changed every day. After 6 days, micro-CT imaging confirmed that the scaffolds were fully decalcified. The samples were then rinsed and stored in sterile PBS at 4°C until cell seeding.

Cell isolation, Seeding, and Culture

Stromal cells were isolated from the femurs and tibias of 30- to 60-day-old female Sprague Dawley rats (Charles River) using a method described by Ishaug et al.[14] NIH guidelines for the care and use of laboratory animals were observed. The stromal cells were cultured in T-150 flasks to passage two and were then cryopreserved in liquid nitrogen with cryogenic media (10% DMSO and 90% fetal bovine serum) until seeding. Calvarial cells were isolated from 24-h-old Sprague Dawley rat pups (Charles River) using a method outlined by Boden et al.[24] The calvarial cells were cultured to passage two and were also cryopreserved until scaffold seeding.

One day prior to scaffold seeding, the stromal and calvarial cells were thawed at 37°C and placed in T-150 flasks with media. The PLDL and demineralized trabecular bone matrix (DTBM) scaffolds (n = 50 each) were wetted with culture media (α-MEM, 10% fetal bovine serum, and 1% penicillin–streptomycin) immediately prior to use, seeded with either 1×10^6 calvarial or 0.5×10^6 stromal cells in 50 μL of media, and incubated at 37°C and 5% CO_2 in six-well plates. After 1 h, 4 mL of culture media was added to each construct. Culture media containing osteoinductive supplements (10^{-8} *M* dexamethasone, 50 μg/mL l-ascorbic acid, and 3 m*M* β-glycerophosphate) was then added after 2 days and then changed every 2 days. The seeding of the two cell types on two different scaffolds gave rise to four analysis groups: DTBM with calvarial cells (DTBM/Cal), DTBM with stromal cells (DTBM/Str), PLDL with calvarial cells (PLDL/Cal),

and PLDL with stromal cells (PLDL/Str). After 1 day, five constructs from each study group were removed for histology and real time quantitative reverse transcription polymerase chain reaction (RT-PCR) analysis. The remaining constructs were cultured for 8 weeks.

Micro-CT imaging

Starting at 4 weeks, one cell-seeded construct from each analysis group was imaged in culture media under sterile conditions with the micro-CT at 16-μm resolution and then returned to *in vitro* culture. From weeks 5 to 8, these same constructs were imaged weekly to monitor mineralization throughout the constructs. Beginning at 5, 6, and 7 weeks, different constructs from each analysis group were introduced and underwent weekly sequential imaging until week 8. Finally, at 8 weeks, all constructs (including constructs that had not been previously scanned) and acellular PLDL and DTBM scaffold controls ($n = 6$ each) were scanned with micro-CT before subsequent analysis of gene expression using real time quantitative RT-PCR and histology.

Histology

At days 1 and 56, samples from each analysis group were stored in 10% formalin solution for 24 h and fixed in 70% ethanol. The samples were then paraffin embedded and sectioned at 5 μm. Toluidine blue (TB), hematoxylin and eosin (HE), Goldner's trichrome (GT), VK, and safranin-O staining and immunohistochemical analysis for types I and II collagen were performed on each sample prior to viewing with a light microscope (Eclipse E800, Nikon).

Real time quantitative RT-PCR

Samples from days 1 ($n = 1$ each) and 56 ($n = 4$ or 5 each) were sliced into small pieces. The RNA was isolated using a Qiagen RNeasy mini kit according to the manufacturer's instructions. The total amount of RNA from each sample was quantified using a UV–visible 1601 spectrophotometer (Shimadzu) with absorbance readings at 260- and 280-nm wavelengths. First strand cDNA synthesis was performed using superscript II and following the procedures described by the manufacturer (Gibco BRL). Real time quantitative RT-PCR was performed utilizing an ABI PRISM 7700 (Applied Biosystems) sequence detector to detect the fluorescence emitted at each PCR amplification. This allowed for quantification to be performed on relative amounts of gene expression from each cell-seeded scaffold under analysis. The osteocalcin (OCN), osteopontin (OPN), osteonectin (ONN), and alkaline phosphatase (ALP) genes were quantified and normalized to 18S.

Statistical analysis

Multiple samples were collected for each measurement and expressed as means ± standard deviations. Multiway analysis of variance (ANOVA) was used to assess the possible interactions between the study groups, the number of scans, the initial scanning time point, and the culture time for the amount of mineralization formed. The data from each sample group were analyzed for statistical significance with a one-way ANOVA test using the Fisher least significance test for *post hoc* comparisons and a significance level of $p < 0.05$. The same ANOVA statistical analysis was performed to evaluate the gene expression differences for the sample groups at 8 weeks.

RESULTS

Micro-CT analysis

At 4 weeks, micro-CT imaging revealed mineralization within all construct groups. Mineralization was present throughout the PLDL constructs but was limited to the periphery of DTBM constructs (Figs. 2, 3). The volume of mineralization within all sequentially imaged constructs continued to increase to 8 weeks in culture as shown in Figures 2 and 4. The mineralized matrix volume (mm^3) was significantly greater ($p < 0.01$) at 8 weeks than at 4, 5, or 6 weeks. The total mineralized matrix volume at 8 weeks was higher ($p < 0.05$) within the DTBM constructs compared to the PLDL constructs for both cell types (Fig. 3); however, mineralization was detected on acellular DTBM scaffolds, indicating partial remineralization of the natural bone extracellular matrix. Histological analysis confirmed the presence of mineralized matrix on the periphery of the acellular DTBM controls. Mineralization was not observed in the PLDL acellular controls. There was no significant effect of cell type on mineralized matrix production (Fig. 5). Moreover, repeated micro-CT scanning did not have a significant influence on the amount of mineralized matrix production.

Quantitative RT-PCR

Stromal and calvarial cells on PLDL and DTBM scaffolds demonstrated definite osteogenic differentiation based on bone-related gene expression for ALP, OCN, ONN, and OPN at 8 weeks (Fig. 6). The cell type had no significant effect on gene expression except for OCN. Regardless of the scaffold type, calvarial cell constructs exhibited higher levels of OCN expression than stromal cell constructs at 8 weeks. The samples consisting of calvarial cells seeded onto PLDL also expressed significantly more ALP, ONN, and OPN

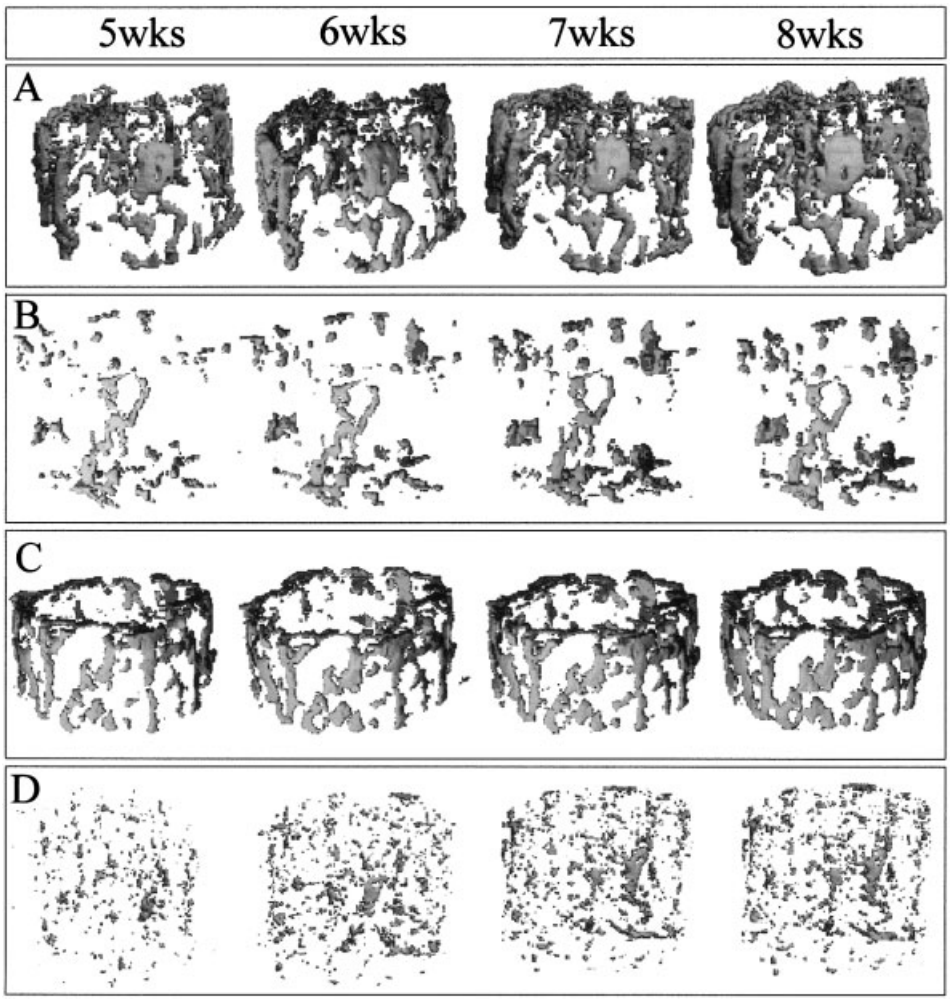

Figure 2. Sequentially scanned micro-CT images of 3D scaffolds of demineralized trabecular bone matrix (DTBM) or PLDL scaffolds plus either rat stromal (Str) or calvarial (Cal) cells at 5, 6, 7, and 8 weeks. (A) DTBM/Str, (B) PLDL/Str, (C) DTBM/Cal, and (D) PLDL/Cal.

genes in comparison to the samples of calvarial cells seeded onto DTBM scaffolds.

Histology

The VK, TB, and GT staining of the 1-day cell-seeded scaffolds showed that cells were present within the interior and that there was no mineralization present initially. The analysis of 1-day constructs also confirmed that the DTBM scaffolds were completely demineralized prior to cell seeding. At 8 weeks, VK and TB staining clearly distinguished differences between cell-mediated mineralization and remineralization of extracellular matrix on the DTBM constructs (Fig. 7). PLDL constructs contained only cell-mediated mineralization (Fig. 8). Additionally, VK and TB staining verified micro-CT analyses showing that mineralization was present throughout the PLDL samples whereas mineralization was localized on the DTBM construct margin. Mineralization produced by calvarial cells was in the form of dense, irregular deposits whereas the stromal cells laid down finely scattered, circular phosphate deposits (Figs. 7, 8). A thick nonmineralized cellular layer overlying the construct periphery was seen in both DTBM/Str and PLDL/Str groups. Staining with HE and GT also illustrated that the stromal cells were embedded within the mineralized matrix. For all DTBM constructs, few cells were detected within the interior of the scaffolds, indicating that the cells present in the 1-day seeded constructs had died or migrated to the periphery. However, there was histological evidence of cells throughout the PLDL constructs.

Immunohistochemical staining for type I collagen was positive for all constructs in areas where VK staining indicated phosphate deposits. Type II collagen expression and safranin-O staining for sGAG was also found in regions of some constructs, but it was not present in the PLDL/Str constructs. VK staining

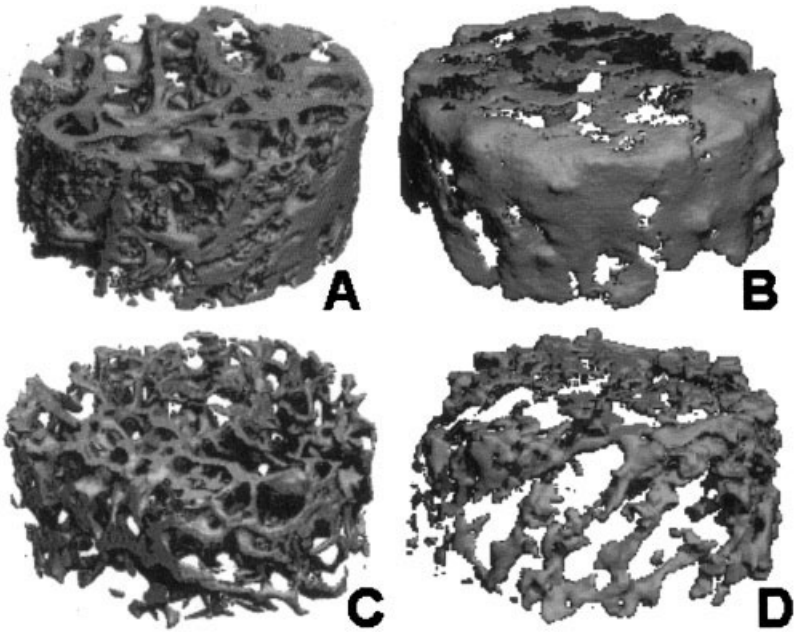

Figure 3. (A) Micro-CT images of undemineralized trabecular scaffold and (B) the same scaffold 8 weeks later after demineralization and incubation with stromal cells. (C) An undemineralized trabecular scaffold and (D) the corresponding calvarial cell seeded DTBM at 8 weeks.

was also positive in some of the regions where type II collagen and sGAG expression were present. As determined from HE, GT, and TB histology, local cells within these regions had a morphology consistent with hypertrophic chondrocytes.

DISCUSSION

This study is the first to demonstrate that micro-CT imaging may be used to monitor mineralized matrix formation within 3D tissue-engineered constructs *in vitro*. An experimental design was employed to test whether repeated micro-CT imaging of constructs influenced cell function. Previous studies have shown that repeated exposure to low-voltage X-ray irradiation inhibited proliferation of vascular smooth muscle and adventitial cells.[25] In this study, weekly sequential micro-CT imaging revealed a consistent increase in total matrix mineralization volume over time in culture, demonstrating that multiple scans did not eliminate the cells' ability to produce mineralized matrix. Furthermore, the multiway ANOVA indicated that repeated scanning did not significantly reduce mineralized matrix formation. Because the micro-CT imaging process was nondestructive, imaged constructs were available for subsequent histological analysis.

The mineralization produced within DTBM con-

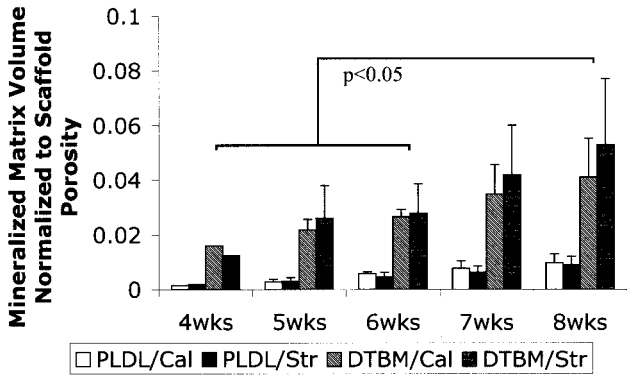

Figure 4. The total mineralized matrix volume on demineralized trabecular bone matrix (DTBM) or PLDL scaffolds plus either rat stromal (Str) or calvarial (Cal) cells as a function of time in culture. Significant differences between groups are indicated for $p < 0.05$.

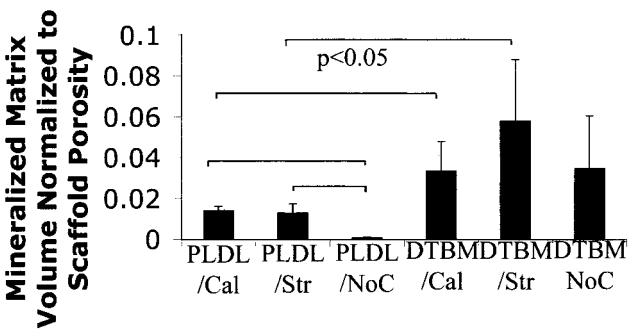

Figure 5. The mineralized matrix volume for demineralized trabecular bone matrix (DTBM) or PLDL scaffolds plus either rat stromal (Str) or calvarial (Cal) cells and acellular scaffolds (NoC, no cells) at 8 weeks. Significant differences between groups are indicated for $p < 0.05$.

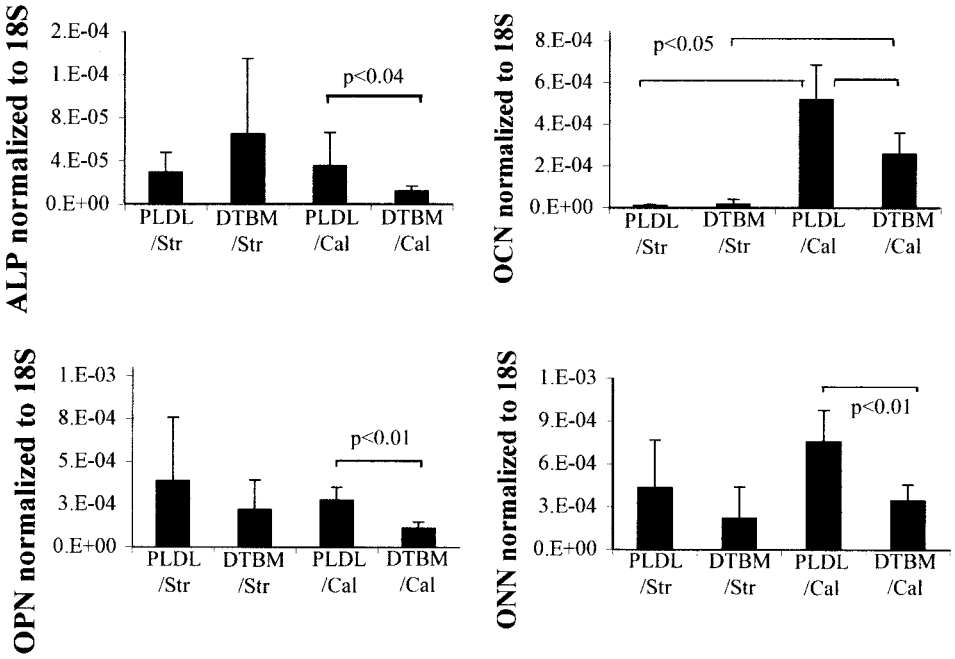

Figure 6. Bone-related marker gene expressions of either rat stromal (Str) or calvarial (Cal) cells seeded on either demineralized trabecular bone matrix (DTBM) or PLDL scaffolds at 8 weeks. ALP, alkaline phosphatase; OCN, osteocalcin; OPN, osteopontin; ONN, osteonectin.

structs was localized along the periphery, which is consistent with previous observations of 3D bone tissue engineered constructs cultured under static conditions.[14,15] Differences in the distribution of mineralization observed within oriented PLDL and DTBM constructs may be attributed to differences in the scaffold microarchitecture. The PLDL macropores may have provided enhanced nutrient diffusion and cellular migration to the scaffold interior, which in turn may explain the mineralization seen throughout the PLDL scaffolds.

Although the total volume of mineralization detected by micro-CT was greater ($p < 0.05$) within DTBM constructs than PLDL constructs, the mineralized matrix volume produced by the cells only (i.e., not including remineralized matrix) was similar between the different scaffold groups. An estimate of the cell-mediated mineralized matrix was obtained by

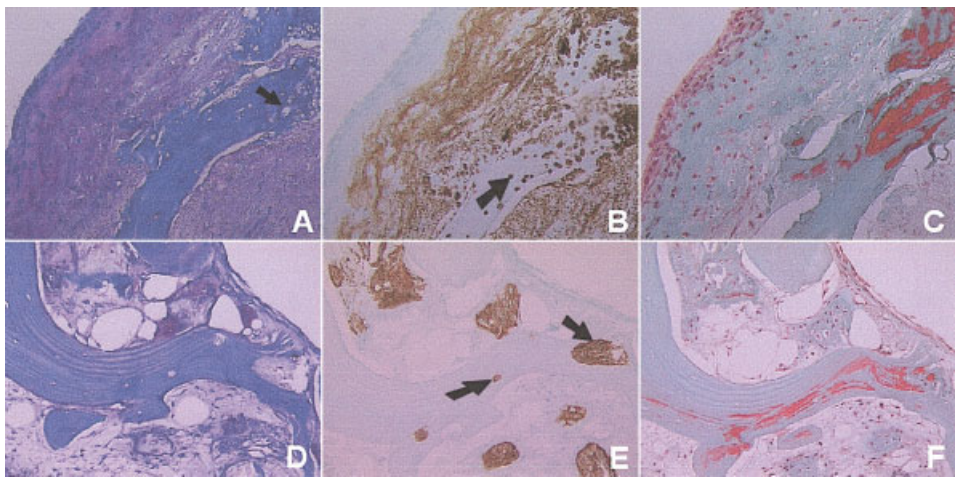

Figure 7. Histological staining of demineralized trabecular bone matrix (DTBM) scaffolds seeded with either rat stromal (Str) or calvarial (Cal) cells at 8 weeks. (A,D) Toluidine blue, (B,E) Von Kossa fast green, and (C,F) Goldner's trichrome staining on (A–C) DTBM/Str at 8 weeks and (D–F) DTBM/Cal at 8 weeks. The arrows denote areas of scaffold remineralization (original magnification ×20). [Color figure can be viewed in the online issue, which is available at www.interscience.wiley.com.]

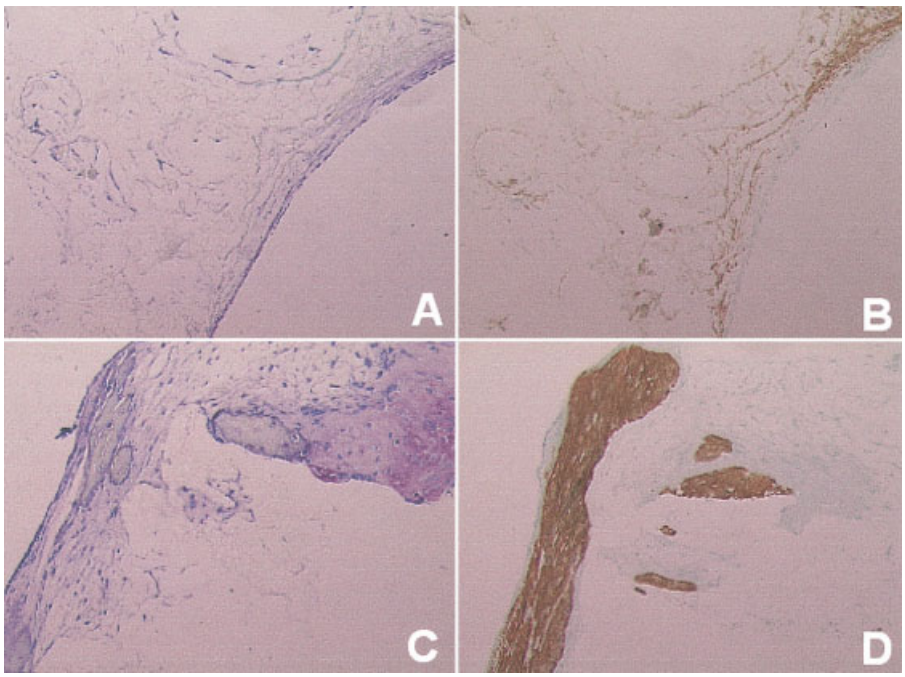

Figure 8. Histological staining of PLDL scaffolds seeded with either rat stromal (Str) or calvarial (Cal) cells at 8 weeks. (A,C) Toluidine blue and (B,D) Von Kossa fast green staining on (A,B) PLDL/Str and (C,D) PLDL/Cal at 8 weeks (original magnification ×20). [Color figure can be viewed in the online issue, which is available at www.interscience.wiley.com.]

subtracting the mineralized volume measured in acellular controls from that in cell-seeded constructs. The VK and TB staining of histological sections clearly distinguished cell-mediated mineralization from remineralization of the DTBM scaffolds. Matrix remineralization appeared to be dense circular-shaped deposits located within the bone matrix, whereas cell-mediated mineralization occurred on the DTBM surfaces.

Safranin-O staining and immunohistochemical analysis for type II collagen indicated that the extracellular matrix formation in DTBM was partly calcified cartilage. The cells within these regions exhibited an appearance consistent with hypertrophic chondrocytes. This suggests that DTBM scaffolds possessed bioactive factors that induced chondrogenic differentiation for both cell types. However, the positive expression of sGAG and type II collagen on PLDL/Cal constructs but not PLDL/Str constructs indicates that the calvarial cell population also contained committed chondrogenic progenitors. This agrees with previous reports that a subset of calvarial cells can express a cartilage phenotype as a result of their 3D environment or the addition of growth factors.[26,27]

The appearance of mineralization and cellular organization on both scaffold types was markedly different between the stromal and calvarial cells. This may be because the stromal cells were a more heterogenous population than the calvarial cells and they may have contained proliferating fibroblasts, which formed the nonmineralized layer on the scaffold periphery.

There was increased bone-related gene expression produced by cells on PLDL compared to DTBM at 8 weeks. OCN is produced late in the osteoblast differentiation pathway just prior to and during mineralization. This may indicate that the cells seeded on PLDL scaffolds were in the initial stages of increasing matrix production. OCN was specifically upregulated in the DTBM/Cal group in comparison to the DTBM/Str group, perhaps reflecting the more advanced differentiation stage of the primary calvarial osteoblasts. The results gained from the micro-CT and the real time PCR correlate, in that there was an upregulation of cell-mediated mineralized matrix production and an upregulation in bone-related gene expression with the PLDL/Cal group at 8 weeks in comparison to the DTBM/Cal group.

CONCLUSION

This study demonstrated that high-resolution micro-CT imaging may be used to nondestructively and quantitatively monitor the temporal progression of mineralized matrix formation within 3D constructs *in vitro*. Repeated scanning (up to 5 times) did not significantly inhibit the function of cells seeded onto trabecular bone or polymeric scaffolds. These methods may be used to efficiently evaluate cells and scaffolds for bone tissue engineering applications *in vitro* prior to preclinical testing. We further conclude that PLDL scaffolds support cell attachment, differentiation, and

cell-mediated mineralization *in vitro* that is comparable to natural DTBM scaffolds. Additional studies are required to evaluate whether the novel oriented microarchitecture of the PLDL scaffolds can facilitate the repair of critically sized bone defects *in vivo*.

This work made use of the ERC Shared Facilities supported by the National Science Foundation. Financial support was also provided from the Wellcome Trust as a Travel Grant. We wish to thank Georgia Tissue Bank for providing the human trabecular bone samples and Tracy Couse for help in performing the histology.

References

1. Boden SD. Biology of lumbar spine fusion and use of bone graft substitutes: present, future, and next generation. Tissue Eng 2000;6:383–399.
2. Khan SN, Sandhu HS, Parvataneni HK, Girardi FP, Cammisa FP Jr. Bone graft substitutes in spine surgery. Bull Hosp Joint Dis 2000;59:5–10.
3. Block JE, Poser J. Does xenogeneic demineralized bone matrix have clinical utility as a bone graft substitute? Med Hypotheses 1995;45:27–32.
4. Hagen JW, Semmelink JM, Klein CP, Prahl-Andersen B, Burger EH. Bone induction by demineralized bone particles: long-term observations of the implant–connective tissue interface. J Biomed Mater Res 1992;26:897–913.
5. Urist MR, Silverman BF, Buring K, Dubuc FL, Rosenberg JM. The bone induction principle. Clin Orthop 1967;53:243–283.
6. Linden GJ. Bone induction in implants of decalcified bone and dentine. J Anat 1975;119:359–367.
7. Toriumi DM, Larrabee WF Jr, Walike JW, Millay DJ, Eisele DW. Demineralized bone. Implant resorption with long-term follow-up. Arch Otolaryngol Head Neck Surg 1990;116:676–680.
8. Groeneveld EH, van den Bergh JP, Holzmann P, ten Bruggenkate CM, Tuinzing DB, Burger EH. Mineralization processes in demineralized bone matrix grafts in human maxillary sinus floor elevations. J Biomed Mater Res 1999;48:393–402.
9. Kaban LB, Mulliken JB, Glowacki J. Treatment of jaw defects with demineralized bone implants. J Oral Maxillofac Surg 1982;40:623–626.
10. Mueller SM, Glowacki J. Age-related decline in the osteogenic potential of human bone marrow cells cultured in three-dimensional collagen sponges. J Cell Biochem 2001;82:583–590.
11. Fuss M, Ehlers EM, Russlies M, Rohwedel J, Behrens P. Characteristics of human chondrocytes, osteoblasts and fibroblasts seeded onto a type I/III collagen sponge under different culture conditions. A light, scanning and transmission electron microscopy study. Anat Anz 2000;182:303–310.
12. Hutmacher DW, Schantz T, Zein I, Ng KW, Teoh SH, Tan KC. Mechanical properties and cell cultural response of polycaprolactone scaffolds designed and fabricated via fused deposition modeling. J Biomed Mater Res 2001;55:203–216.
13. Holy CE, Shoichet MS, Davies JE. Engineering three-dimensional bone tissue *in vitro* using biodegradable scaffolds: investigating initial cell-seeding density and culture period. J Biomed Mater Res 2000;51:376–382.
14. Ishaug SL, Crane GM, Miller MJ, Yasko AW, Yaszemski MJ, Mikos AG. Bone formation by three-dimensional stromal osteoblast culture in biodegradable polymer scaffolds. J Biomed Mater Res 1997;36:17–28.
15. Ishaug-Riley SL, Crane-Kruger GM, Yaszemski MJ, Mikos AG. Three-dimensional culture of rat calvarial osteoblasts in porous biodegradable polymers. Biomaterials 1998;19:1405–1412.
16. Lisignoli G, Zini N, Remiddi G, Piacentini A, Puggioli A, Trimarchi C, Fini M, Maraldi NM, Facchini A. Basic fibroblast growth factor enhances *in vitro* mineralization of rat bone marrow stromal cells grown on non-woven hyaluronic acid based polymer scaffold. Biomaterials 2001;22:2095–2105.
17. Fisher JP, Holland TA, Dean D, Engel PS, Mikos AG. Synthesis and properties of photocross-linked poly(propylene fumarate) scaffolds. J Biomater Sci Polym Ed 2001;12:673–687.
18. Hasegawa Y, Ohgushi H, Ishimura M, Habata T, Tamai S, Tomita N, Ikada Y. Marrow cell culture on poly-l-lactic acid fabrics. Clin Orthop 1999:235–243.
19. Lin ASP, Barrows TH, Cartmell SH, Guldberg RE. Microarchitectural and mechanical characterization of orientated porous polymer scaffolds. Biomaterials 2003;24:481–489.
20. Ishaug-Riley SL, Crane GM, Gurlek A, Miller MJ, Yasko AW, Yaszemski MJ, Mikos AG. Ectopic bone formation by marrow stromal osteoblast transplantation using poly(dl-lactic-*co*-glycolic acid) foams implanted into the rat mesentery. J Biomed Mater Res 1997;36:1–8.
21. Kuhn JL, Goldstein SA, Feldkamp LA, Goulet RW, Jesion G. Evaluation of a microcomputed tomography system to study trabecular bone structure. J Orthop Res 1990;8:833–842.
22. Guldberg RE, Caldwell NJ, Guo XE, Goulet RW, Hollister SJ, Goldstein SA. Mechanical stimulation of tissue repair in the hydraulic bone chamber. J Bone Miner Res 1997;12:1295–1302.
23. Richards M, Goulet JA, Schaffler MB, Goldstein SA. Temporal and spatial characterization of regenerate bone in the lengthened rabbit tibia. J Bone Miner Res 1999;14:1978–1986.
24. Boden SD, Hair G, Titus L, Racine M, McCuaig K, Wozney JM, Nanes MS. Glucocorticoid-induced differentiation of fetal rat calvarial osteoblasts is mediated by bone morphogenetic protein-6. Endocrinology 1997;138:2820–2828.
25. Scott NA, Crocker IR, Yin Q, Sorescu D, Wilcox JN, Griendling KK. Inhibition of vascular cell growth by X-ray irradiation: comparison with gamma radiation and mechanism of action. Int J Radiat Oncol Biol Phys 2001;50:485–493.
26. Asahina I, Sampath TK, Nishimura I, Hauschka PV. Human osteogenic protein-1 induces both chondroblastic and osteoblastic differentiation of osteoprogenitor cells derived from newborn rat calvaria. J Cell Biol 1993;123:921–933.
27. Basic N, Basic V, Bulic K, Grgic M, Kleinman HK, Luyten FP, Vukicevic S. TGF-beta and basement membrane matrigel stimulate the chondrogenic phenotype in osteoblastic cells derived from fetal rat calvaria. J Bone Miner Res 1996;11:384–391.